

# Characterization and mechanism study of micrometer-sized secondary assembly of $\beta$ -cyclodextrin

Yifeng He, Xinghai Shen,\* Qingde Chen and Hongcheng Gao

Received 16 June 2010, Accepted 1 September 2010

DOI: 10.1039/c0cp00899k

We herein report a  $\beta$ -cyclodextrin-based secondary assembly ( $\beta$ -CD SA) obtained from an aqueous solution. It was found that the addition of a very small amount of organic molecule 2-phenyl-5-(4-diphenyl) 1,3,4-oxadiazole (PBD) into an aqueous solution of 10 mM  $\beta$ -CD led to the formation of a micrometer-sized rodlike SA, which made the mixture turbid immediately. After careful characterization, the structure and the formation mechanism of the  $\beta$ -CD SA were suggested. PBD first induces  $\beta$ -CDs to form rigid nanotubes through head-to-head or tail-to-tail routes. Using the “solid” nanotubes as recrystallization centers, other  $\beta$ -CDs assembled to channel in the  $c$  axis direction and hexagonally aligned in the  $b$  axis direction, leading to the formation of a  $\beta$ -CD SA. In the  $\beta$ -CD SA, most of the  $\beta$ -CDs were not occupied by PBD. In the course of formation, intermolecular hydrogen-bonding plays a prominent role. The results reported herein would be helpful in constructing cyclodextrin-based architectures in water.

## Introduction

Self-assembly is a very powerful way of building large-sized and complicated architectures, which could not be directly synthesized by conventional covalent methods.<sup>1</sup> It is the autonomous organization of components into patterns or structures occurring mainly through noncovalent interactions such as van der Waals forces, hydrogen-bonding, hydrophilic/hydrophobic interactions, electrostatic interactions, donor and acceptor interactions, and metal–ligand coordination networks.<sup>2</sup> Manipulation of the structures in self-organizing materials is critically important in achieving the desired functions and properties of molecular materials. Thus, diverse molecular architectures have been explored as a means to manipulate supramolecular structures and have a dramatic effect on their physical properties.<sup>3</sup>

A great number of organic molecules have been designed and synthesized to construct nanometer and even micrometer supramolecular structures, which are of fundamental and technological importance due to their unique properties for applications in chemistry, material science, life science and nanotechnology.<sup>4</sup> Using an amphiphilic hyperbranched copolymer as a building block, a tubular structure with macroscopic dimensions was first prepared through self-assembly.<sup>5</sup> Among the driving forces, hydrogen-bonding plays a prominent role in supramolecular chemistry because of its directionality and versatility. Additionally, if a new phase such as a solid phase appears in an aqueous solution, hydrogen-bonding would be enforced by phase separation.<sup>6</sup>

Not only synthetic molecules but also natural or semi-natural molecules have been used more and more to construct supramolecular architectures. For example, cyclodextrins (CDs), which have a hydrophobic cavity and many hydroxyl groups on the primary and secondary faces, have received much attention partly due to the formation of ordered and functionalized assemblies.<sup>7,8</sup> Their hydroxyl groups favor the formation of both intramolecular and intermolecular hydrogen-bonds. This makes it possible to form complex aggregates. Some organic molecules have been employed to build CD-based nanotubes.<sup>9,10</sup> For instance, Li and McGown found that  $\beta$ - and  $\gamma$ -CD molecules could be linked by strings of diphenylhexatriene (DPH) molecules to form nanotubes in solution.<sup>9a</sup> Agbaria and Gill reported that some oxazole molecules including 2-phenyl-5-(4-diphenyl) 1,3,4-oxadiazole (PBD) can form inclusion complexes with  $\gamma$ -CD at lower concentrations and these inclusion complexes can form extended nanotubes at relatively high concentrations.<sup>9b,c</sup> Evidence for this is visible turbidity after mixing an equimolar solution of  $\gamma$ -CD with PBD.<sup>9b,c</sup> Later, we also found the similar phenomenon happened to PBD interacting with  $\beta$ -CD.<sup>10,11</sup> Further investigation suggested for the first time that the turbidity observed in the PBD/ $\beta$ -CD system originated from the secondary assembly (SA) of  $\beta$ -CD nanotubes.<sup>10a,11</sup> It was also found that most  $\beta$ -CDs in the  $\beta$ -CD SA were unoccupied by PBD.<sup>11</sup> Very recently,  $\alpha$ -CD and  $\gamma$ -CD nanotubular superstructures similar to  $\beta$ -CD SA have also been reported.<sup>12,13</sup> However, the microstructure and formation mechanism of the SA have not been made clear so far.

In this work, we employ steady and transient state fluorescence, wide-angle X-ray diffraction (WAXRD), field-emission scanning electron microscopy (FESEM), high-resolution transmission electron microscopy (HRTEM), Fourier transform infrared (FTIR), and  $N_2$  adsorption–desorption isotherms to characterize the  $\beta$ -CD SA. The structural features and formation mechanism of the  $\beta$ -CD SA are therefore suggested. As a

Beijing National Laboratory for Molecular Sciences (BNLMS), Radiochemistry and Radiation Chemistry Key Laboratory of Fundamental Science, College of Chemistry and Molecular Engineering, Peking University, Beijing 100871, China. E-mail: xshen@pku.edu.cn; Fax: 86-10-62759191; Tel: 86-10-62765915

“bottom-up” strategy, the above results may open up the possibility of creating novel and functional materials from CDs with self-assembly.

## Experimental section

### Materials

$\beta$ -CD (Fine Chemical Products of Nankai University, China) was recrystallized twice using tridistilled water and dried under vacuum for 24 h. PBD (Acros, 99%) and ethanol (HPLC, Tianjin Siyou) were used as received. Tridistilled water was used throughout the experiments. All other chemical reagents used in this study were of analytical grade.

### Samples

A stock solution of PBD ( $10^{-3}$  M) was prepared in ethanol. In order to prepare  $\beta$ -CD SA, the following procedures were performed: (1) 5 mL of stock solution of PBD was added to a 500 mL volumetric flask; (2) 10 mM of  $\beta$ -CD aqueous solution was added to give a certain volume, *i.e.*, 500 mL. The final concentration of PBD was  $1 \times 10^{-5}$  M; (3) the obtained mixture was sonicated for 1 h, and then incubated for 12 h; (4) after that, dispersed products ( $\beta$ -CD SA) were collected by centrifugation ( $12\,000\text{ r min}^{-1}$ ) and dried in a vacuum oven at  $40\text{ }^{\circ}\text{C}$  for 24 h.

### Measurements

Fluorescence spectra were obtained using a FL-4500 (Hitachi, Japan) spectrofluorimeter. Fluorescence lifetime measurements were made on a multiplexed time-correlated single-photon counting fluorimeter FLS920 (EDINBURGH), and 3000 counts were collected for each sample. The lifetime value was determined from data on the fluorescence transient waveform of the material to be tested and the lamp waveform data using the least-squares iterative deconvolution method. All the fluorescence spectra and fluorescence lifetime were measured under air atmosphere at room temperature, and the excitation wavelength was 310 nm. The fluorescence spectra were normalized by the maximum emission intensity in each spectrum. With respect to the solid fluorescence measurement, the solid samples were ground in an agate mortar and then added into the sample cell. WAXRD patterns were obtained at room temperature on a DMAX-2400 (Rigaku, Japan) diffractometer with a  $\text{Cu K}\alpha$  radiation source ( $\lambda = 0.154041\text{ nm}$ ). The supplied voltage and current were set to 40 kV and 100 mA, respectively. Powder samples were mounted on a sample holder and scanned from  $3^{\circ}$  to  $40^{\circ}$  of  $2\theta$  at a speed of  $5^{\circ}\text{ min}^{-1}$ . FTIR spectra were recorded on a Bruker Vector22 spectrometer at frequency ranging from 400 to  $4000\text{ cm}^{-1}$ . Micrographs of HRTEM were recorded with Tecnai-F30 by the negative staining method. One drop of the sample solution was placed onto a formvar-coated copper grid, and a uranyl acetate solution (2%) was used as the staining agent. The morphologies of the samples were also visualized by FESEM (Hitachi, S-4800).  $\text{N}_2$  adsorption-desorption isotherms were determined on a Micromeritics ASAP-2010 apparatus at 77 K. Prior to the measurement, after being ground in an agate mortar, all the samples were

loaded in the sample cell, and heated at  $120\text{ }^{\circ}\text{C}$  and  $10^{-6}$  Torr for 4 h to remove hygroscopic water completely. The surface areas of the samples were calculated with the Brunauer–Emmett–Teller (BET) equation, while their pore size distributions and cumulative surface areas of the pores were determined by the Barrett–Joyner–Halenda (BJH) analyses on the desorption branch.

## Results and discussion

### Fluorescence measurement

Fig. 1 shows the fluorescence spectra of  $10^{-5}$  M PBD in water,  $10^{-5}$  M PBD and 10 mM  $\beta$ -CD in water, solid PBD, and the solid  $\beta$ -CD SA. Compared with the fluorescence spectra of  $10^{-5}$  M PBD in water, the addition of 10 mM  $\beta$ -CD results in a hypsochromic shift of 5 nm at the maximum peak from 378.4 to 373.4 nm, since  $\beta$ -CD accommodates PBD to form nanotubes.<sup>10b</sup> Similarly, by comparing the spectra of solid PBD and the solid  $\beta$ -CD SA, it is not difficult to see that PBD does exist in the structure of the  $\beta$ -CD SA and the formation of the  $\beta$ -CD SA leads to a considerable hypsochromic shift of 24.8 nm of the maximum peak from 391.8 to 367 nm. In the previous work, we found that the mixture of PBD ( $10^{-5}$  M) and  $\beta$ -CD (10 mM) in water was turbid while individual solutions of PBD ( $10^{-5}$  M) or  $\beta$ -CD (10 mM) were clear.<sup>10b</sup> Furthermore, a SA of  $\beta$

may come from the different environment around a PBD molecule. In a PBD solid, a PBD molecule exists in a crystal lattice, which is relatively rigid; while in a  $\beta$ -CD SA, it exists in a cavity of  $\beta$ -CD, which is relatively flexible.

### WAXRD measurement

Crystalline structures of PBD,  $\beta$ -CD and the  $\beta$ -CD SA have been studied using WAXRD. As shown in Fig. 2, the three samples have well crystallization according to their well patterns. Major peaks at  $2\theta = 9.5^\circ$ ,  $12.8^\circ$ ,  $13.4^\circ$ , and  $18.2^\circ$  are observed in the  $\beta$ -CD pattern, indicating the existence of a typical cage structure.<sup>15</sup> There is no obvious diffraction peak of PBD in the  $\beta$ -CD SA which may imply that the quantity of PBD is very small in the  $\beta$ -CD SA. In fact, previous density measurements also confirmed that most  $\beta$ -CDs in the  $\beta$ -CD SA were empty and not occupied by PBD.<sup>11</sup> The  $\beta$ -CD SA has a different pattern relative to  $\beta$ -CD, with main signals at  $11.76^\circ$  and  $17.84^\circ$ , indicating the formation of a head-to-head channel-type structure.<sup>15c</sup> This structure is considerably different from that of  $\beta$ -CD.<sup>15</sup> Topchieva *et al.* reported the channel structures and the related WAXRD profiles.<sup>16</sup> Kwak *et al.* also synthesized a self-assembly of  $\alpha$ -CD in which the  $\alpha$ -CDs were closely packed in the vertical direction and hexagonally aligned in the horizontal direction.<sup>17</sup> According to the WAXRD profiles, a schematic illustration of channel-type crystalline structures of the  $\alpha$ -CD SA was suggested.<sup>17a</sup> Similarly, according to the WAXRD pattern of the  $\beta$ -CD SA, we suggest a possible microstructure in Fig. 3 and the corresponding peaks are also indicated in Fig. 2. Major peaks at  $2\theta = 5.84^\circ$  ( $d = 15.12 \text{ \AA}$ ),  $6.44^\circ$  ( $d = 13.71 \text{ \AA}$ ),  $10.86^\circ$  ( $d = 8.14 \text{ \AA}$ ),  $11.76^\circ$  ( $d = 7.52 \text{ \AA}$ ),  $17.84^\circ$  ( $d = 4.97 \text{ \AA}$ ),  $19.54^\circ$  ( $d = 4.54 \text{ \AA}$ ), and  $21.92^\circ$  ( $d = 4.05 \text{ \AA}$ ) in the  $\beta$ -CD SA pattern are ascribed to the reflection (001), (100), (110), (002), (210), (300) and (220). A HRTEM image of the  $\beta$ -CD SA (Fig. 3c) indicates that the rods are stacked by small nanotubes in a layer-by-layer way along with  $a$  axis direction. In the present work, we present a detailed structural model in Fig. 3b.

### FTIR measurements

It has been demonstrated that FTIR is sensitive to the change in hydrogen-bonding. Fig. 4 shows the FTIR spectra of PBD,

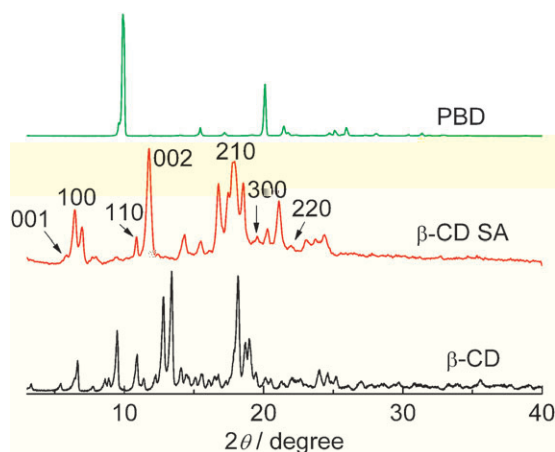


Fig. 2 WAXRD patterns of PBD,  $\beta$ -CD and the  $\beta$ -CD SA.

$\beta$ -CD and the  $\beta$ -CD SA. There is no obvious signal of PBD in the  $\beta$ -CD SA and the spectrum of the  $\beta$ -CD SA is very similar to that of  $\beta$ -CD, indicating that the amount of PBD in the  $\beta$ -CD SA is very small. This is consistent with the analysis of the WAXRD pattern. The spectrum of pure  $\beta$ -CD shows a broad band at  $3389 \text{ cm}^{-1}$ , which is assigned to symmetric and anti-symmetric O–H stretching modes.<sup>18</sup> It shifts to a lower frequency at  $3372 \text{ cm}^{-1}$  because of the formation of the  $\beta$ -CD SA. It is well known that the association of OH groups makes the stretching peak shift to a lower frequency. The difference spectrum of  $\beta$ -CD SA and  $\beta$ -CD shows both positive and negative absorbance peaks at around  $3380 \text{ cm}^{-1}$ , which clearly reflects the association of OH groups. Furthermore, a similar phenomenon also appears at around  $1030 \text{ cm}^{-1}$ , which may be due to OH groups affecting the C–O stretch of  $\beta$ -CD. Thus, the above phenomena confirm the stacking mode of  $\beta$ -CD SA, in which much intermolecular hydrogen bonding between  $\beta$ -CDs exists.

### FESEM images

To further investigate the change in structure from  $\beta$ -CD to the  $\beta$ -CD SA, their morphologies were investigated with FESEM. As shown in Fig. 5, the morphology of  $\beta$ -CD SA is quite different from that of  $\beta$ -CD. The  $\beta$ -CD SA exhibits good crystallization in micrometer-sized rod-like shapes (Fig. 5a), while in pure  $\beta$ -CD there exists much agglomeration without a specific shape resulting from the cage-type crystalline structure (Fig. 5b). These results are consistent with the results of the crystallographic study of the  $\beta$ -CD SA as mentioned above, which suggests the presence of a channel-type crystalline structure with the horizontally hexagonal alignment and the vertically ordered stacking of  $\beta$ -CD.

### $\text{N}_2$ adsorption–desorption isotherm experiment

In order to investigate the structure of the  $\beta$ -CD SA,  $\text{N}_2$  adsorption–desorption isotherm experiments were performed. Both the  $\beta$ -CD SA and  $\beta$ -CD show typical Type I isotherms as illustrated in Fig. 6. Moreover, they show open loop hysteresis, indicating the presence of pore structures.<sup>19</sup> According to BJH analyses of the desorption curves, the average pore size of the  $\beta$ -CD SA is about  $15.7 \text{ nm}$ , close to that of neat  $\beta$ -CD ( $18.5 \text{ nm}$ ). However, the BET surface area and cumulative surface area of pores of the  $\beta$ -CD SA were found to be  $13.2$  and  $12.3 \text{ m}^2 \text{ g}^{-1}$ , respectively, much higher than those of neat  $\beta$ -CD ( $2.2$  and  $1.8 \text{ m}^2 \text{ g}^{-1}$ ). In other words, there are more pore structures in the  $\beta$ -CD SA. Thus,  $\beta$ -CD SA may be a promising candidate for use in the catalysis field instead of  $\beta$ -CD.

### Formation mechanism of $\beta$ -CD SA

According to all of the above results as well as those reported in the literature,<sup>17a</sup> we suggest herein a possible structural model for the  $\beta$ -CD SA (see Fig. 3). In this model,  $\beta$ -CDs are arranged to channel through head-to-head or tail-to-tail routes in the direction of the  $c$  axis and the  $\beta$ -CD channels are hexagonally aligned in the direction of the  $b$  axis. Many such units are arranged along the direction of the  $a$  axis leading to the formation of a micrometer-sized assembly.

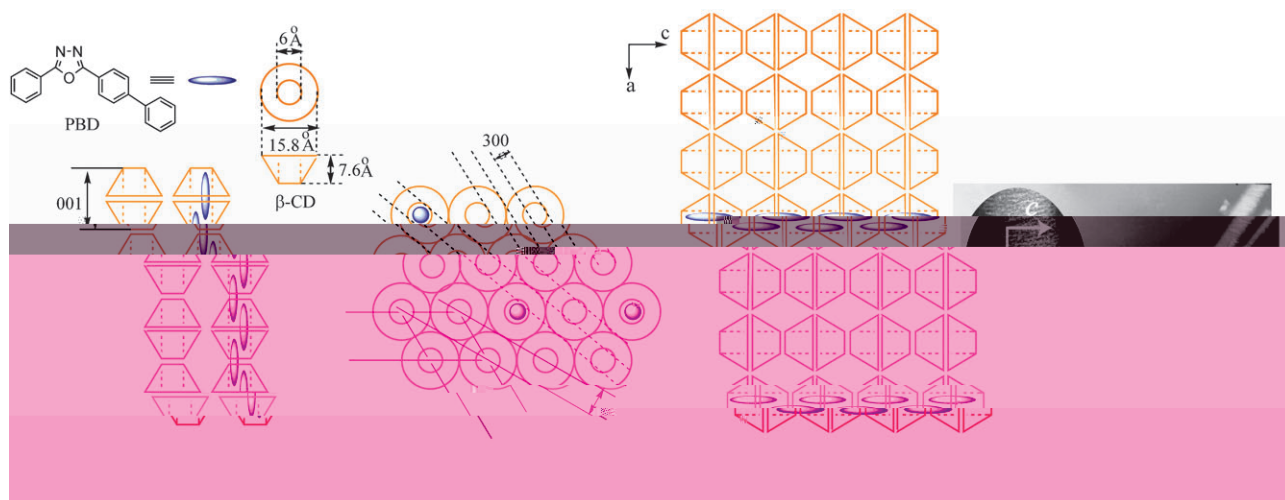


Fig. 3 Schematic illustration of the hierarchical structure of the  $\beta$ -CD SA: (a) and (b). HRTEM micrograph of the micrometer-sized rodlike structure of the  $\beta$ -CD SA: (c).

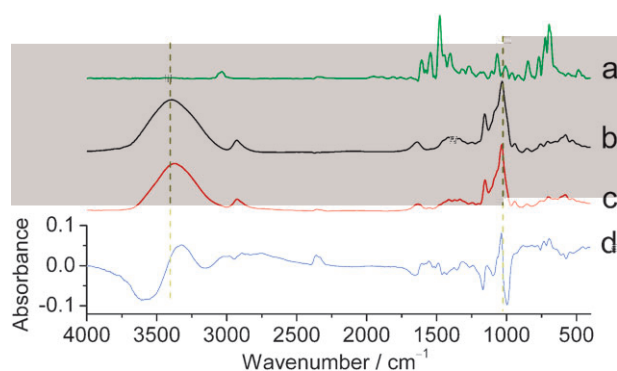


Fig. 4 FTIR absorption spectra of PBD (a),  $\beta$ -CD (b),  $\beta$ -CD SA (c) and difference spectrum (d) obtained from “(c)  $- 1.6 \times$  (b)”.

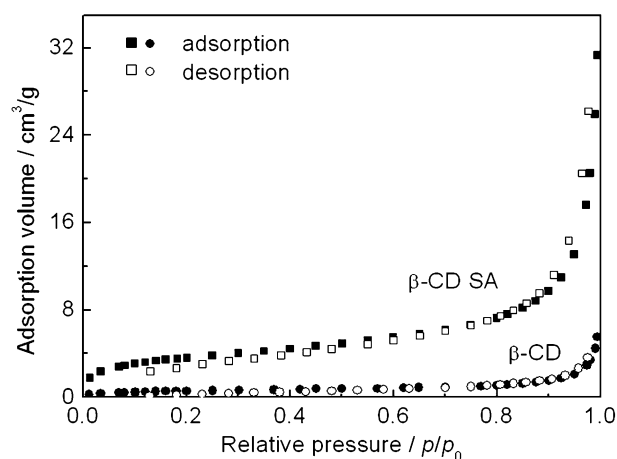


Fig. 6  $N_2$  adsorption-desorption isotherms of  $\beta$ -CD SA and  $\beta$ -CD.

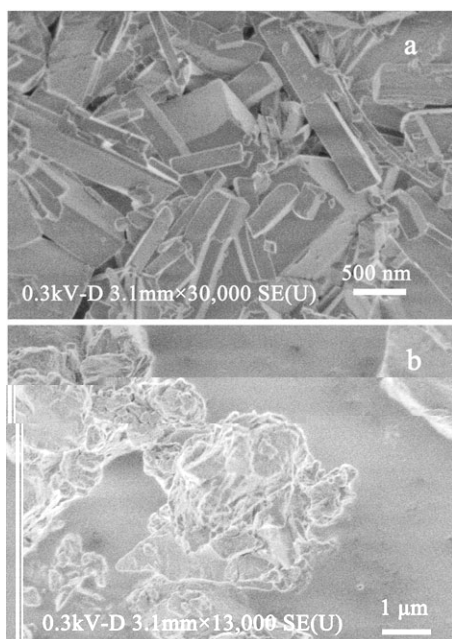


Fig. 5 FESEM images of  $\beta$ -CD SA (a) and  $\beta$ -CD (b).

It is noticeable that  $\beta$ -CD itself can form aggregates in its aqueous solution, which was reported by many research groups.<sup>7,10a,20</sup> Coleman *et al.* proposed a rod-like structure for the aggregates consisting of two chains of hydrated  $\beta$ -CD molecules.<sup>20f</sup> Using CD assemblies as templates to produce mesoporous silica, Polarz *et al.* found wormlike structures and thus suggested that the cyclodextrin aggregate was therefore a bicontinuous “worm-type” pore system with a diameter of about 1.5 nm. Combining a semiempirical CNDO method, they believed that the cyclodextrin complexes preferred to line up in ideally a parallel or staggered parallel arrangement with quadrupolar character.<sup>20e</sup> Becheri *et al.* investigated the formation processes of polypseudorotaxanes based on CDs and polymer like polyethylene-glycol (PEG) or polypropylene-glycol (PPG) and suggested that a preassembled, wormlike aggregate made up of several aligned CDs existed in aqueous solution.<sup>21</sup>

When PBD was added to the aqueous solution of  $\beta$ -CD, it interacts with  $\beta$ -CD to form rigid “solid” PBD- $\beta$ -CD nanotubes. The wormlike-rod structures existing in the aqueous solution of  $\beta$ -CD, and other free  $\beta$ -CD favorably aggregate to



form channels through head-to-head or tail-to-tail routes in the *c* axis direction and align hexagonally in the *b* axis direction using the “solid” nanotubes as recrystallization centers. More and more  $\beta$ -CDs aggregate together and the micrometer-sized assembly is formed. Therefore, when PBD is added, the aqueous solution of  $\beta$ -CD turns turbid. The formation of the  $\beta$ -CD SA is not a one-step process because some intermediate state exists in the formation process. The proof comes from the DLS experiment on the PBD- $\beta$ -CD system, where a new peak with mean hydrodynamic radius around 11 nm appears compared with the sole  $\beta$ -CD system.<sup>11</sup>

In the formation of this micrometer-sized rodlike  $\beta$ -CD SA, intermolecular hydrogen-bonding of  $\beta$ -CDs plays a key role. In the literature, it was reported that a relatively weak hydrogen-bond interaction in the chain extension of conventional polymers can be strengthened by phase separation, for example, crystal formation.<sup>6</sup> In the present study,  $\beta$ -CD nanotubes may be similar to some extent to those polymers induced by hydrogen-bonding.<sup>22</sup> The formation of precipitates in the mixed system results in the appearance of two phases, *i.e.*, phase separation, which leads to the enforcement of the hydrogen-bonds between CDs and favors the formation of the  $\beta$ -CD SA.

In recent years, covalent and noncovalent tubular assemblies with a channel structure based on CDs have been widely reported because they have the potential to be used as nanoscopic filters, biosensors, catalysts, and photoresponsive materials.<sup>16a,b,17a,23a</sup> Covalent tubular assemblies have been obtained by cross-linking the adjacent CDs in a polyrotaxane with epichlorohydrin and the subsequent removal of the included polymeric guest.<sup>23a</sup> Using a similar method, Liu *et al.* reported nanometer-scaled bis( $\beta$ -CD-based molecular tubes) possessing many coordinated metal centers.<sup>24</sup> Noncovalent tubular assemblies have also been constructed by removing the included polymer from a polyrotaxane under the action of a selective organic solvent that is inert in relation to CD.<sup>16a,23c,b</sup> Tonelli *et al.* have reported the tubular CD assemblies by recrystallization of CD using a solvent-nonsolvent system.<sup>23b</sup> Recently, Kwak *et al.* have obtained guest-free  $\alpha$ -CD self-assembly *via* the sonication of  $\alpha$ -CD in tetrahydrofuran.<sup>17a</sup> Here, we suggest another effective method to construct a SA of CD in the absence of an organic solvent and polymer.

## Conclusions

After the careful characterization by steady and transient state fluorescence, WAXRD, FESEM, HRTEM, FTIR, and N<sub>2</sub> adsorption-desorption isotherm, the structure and the formation mechanism of  $\beta$ -CD SA were suggested. PBD first induces  $\beta$ -CDs to form rigid nanotubes, in which  $\beta$ -CDs are arranged to channel through head-to-head or tail-to-tail routes. Using the “solid” nanotubes as recrystallization centers, other  $\beta$ -CDs are packed to channel through head-to-head or tail-to-tail routes in the *c* axis direction and hexagonally aligned in the *b* axis direction. More and more  $\beta$ -CDs deposit together and the micrometer-sized assembly is finally formed. The formation of this micrometer-sized rodlike SA is mainly driven by intermolecular hydrogen-bonding, which is enforced by phase

separation. It is believed that the results reported herein would be helpful in constructing CD-based architectures in water. Besides, these assemblies may act as promising candidates for nanoscopic filters, biosensors, catalysts, and photoresponsive materials.

## Acknowledgements

We are grateful for the financial support from the National Natural Science Foundation of China (Grant No. 20871009). We thank Professor Shifu Weng and Miss Jingjing Zhang for their help with the IR difference spectrum.

## References

- (a) J. M. Lehn, *Angew. Chem., Int. Ed. Engl.*, 1990, 29, 1304–1319; (b) D. Philp and J. F. Stoddart, *Angew. Chem. Int. Ed.*, 1996, 35, 1155–1196.
- G. M. Whitesides and B. Grzybowski, *Science*, 2002, 295, 2418–2421.
- M. Lee, B. K. Cho, Y. S. Kang and W. C. Zin, *Macromolecules*, 1999, 32, 8531–8537.
- (a) Y. Yamamoto, T. Fukushima, Y. Suna, N. Ishii, A. Saeki, S. Seki, S. Tagawa, M. Taniguchi, T. Kawai and T. Aida, *Science*, 2006, 314, 1761–1764; (b) K. Takazawa, Y. Kitahama, Y. Kimura and G. Kido, *Nano Lett.*, 2005, 5, 1293–1296; (c) J. S. Hu, Y. G. Guo, H. P. Liang, L. J. Wan and L. Jiang, *J. Am. Chem. Soc.*, 2005, 127, 17090–17095; (d) H. B. Fu, D. B. Xiao, J. N. Yao and G. Q. Yang, *Angew. Chem., Int. Ed.*, 2003, 42, 2883–2886; (e) A. de la Escosura, M. V. Martinez-Diaz, P. Thordarson, A. E. Rowan, R. J. M. Nolte and T. Torres, *J. Am. Chem. Soc.*, 2003, 125, 12300–12308; (f) J. J. Chiu, C. C. Kei, T. P. Perng and W. S. Wang, *Adv. Mater.*, 2003, 15, 1361–1364; (g) X. J. Zhang, X. H. Zhang, B. Wang, C. Y. Zhang, J. C. Chang, C. S. Lee and S. T. Lee, *J. Phys. Chem. C*, 2008, 112, 16264–16268; (h) G. D. Santos, P. Pengo and J. K. M. Sanders, *Angew. Chem., Int. Ed.*, 2007, 46, 194–197; (i) Y. K. Che, A. Datar, K. Balakrishnan and L. Zang, *J. Am. Chem. Soc.*, 2007, 129, 7234–7235.
- D. Y. Yan, Y. F. Zhou and J. Hou, *Science*, 2004, 303, 65–67.
- L. Brunsveld, B. J. B. Folmer, E. W. Meijer and R. P. Sijbesma, *Chem. Rev.*, 2001, 101, 4071–4097.
- Y. F. He, P. Fu, X. H. Shen and H. C. Gao, *Micron*, 2008, 39, 495–516.
- (a) R. Breslow and S. D. Dong, *Chem. Rev.*, 1998, 98, 1997–2011; (b) G. Wenz, B. H. Han and A. Muller, *Chem. Rev.*, 2006, 106, 782–817; (c) S. A. Nepogodiev and J. F. Stoddart, *Chem. Rev.*, 1998, 98, 1959–1976; (d) A. Harada, Y. Takashima and H. Yamaguchi, *Chem. Soc. Rev.*, 2009, 38, 875–882.
- (a) G. Li and L. B. McGown, *Science*, 1994, 264, 249–251; (b) R. A. Agbaria and D. Gill, *J. Phys. Chem.*, 1988, 92, 1052–1055; (c) R. A. Agbaria and D. Gill, *J. Photochem. Photobiol., A*, 1994, 78, 161–167; (d) A. Harada, J. Li and M. Kamachi, *Nature*, 1992, 356, 325–327; (e) G. Pistolis and A. Malliaris, *J. Phys. Chem.*, 1996, 100, 15562–15568; (f) G. Pistolis and A. Malliaris, *J. Phys. Chem. B*, 1998, 102, 1095–1101; (g) D. Roy, S. K. Mondal, K. Sahu, S. Ghosh, P. Sen and K. Bhattacharyya, *J. Phys. Chem. A*, 2005, 109, 7359–7364; (h) X. H. Wen, M. Guo, Z. Y. Liu and F. Tan, *Chem. Lett.*, 2004, 33, 894–895; (i) X. L. Cheng, A. H. Wu, X. H. Shen and Y. K. Zhang, *Chem. Lett.*, 2004, 33, 894–895.

- 13 P. Das, A. Mallick, D. Sarkar and N. Chattopadhyay, *J. Phys. Chem. C*, 2008, 112, 9600–9603.
- 14 M. R. di Nunzio, P. L. Gentili, A. Romani and G. Favaro, *Chem. Phys. Lett.*, 2010, 491, 80–85.
- 15 (a) H. Jiao, S. H. Goh and S. Valiyaveetil, *Macromolecules*, 2002,